



# Data report: X-ray fluorescence scanning of sediment cores, IODP Expedition 401 Site U1610, Gulf of Cádiz, Atlantic<sup>1</sup>

## Contents

- 1 Abstract
- 1 Introduction
- 3 Methods
- 4 Results
- 6 Data availability
- 6 Acknowledgments
- 7 References

## Keywords

International Ocean Discovery Program, IODP, *JOIDES Resolution*, Expedition 401, Mediterranean–Atlantic Gateway Exchange, Site U1610, Mediterranean Outflow Water, Messinian Salinity Crisis

## References (RIS)

### MS 401-203

Received 21 June 2025

Accepted 4 November 2025

Published 12 February 2026

Xunhui Xu,<sup>2</sup> Jonathan Stine,<sup>2</sup> Patricia Standing,<sup>2</sup> F. Javier Hernández-Molina,<sup>2</sup> Isabelle Billy,<sup>3</sup> Shamar Chin,<sup>2</sup> Sarah J. Feakins,<sup>2</sup> Zhiyang Li,<sup>2</sup> Madeline Mulligan,<sup>4</sup> Danielle Noto,<sup>2</sup> Fadl Raad,<sup>2</sup> Manuel Teixeira,<sup>2</sup> Jesse Yeon,<sup>5</sup> Mohamed Z. Yousfi,<sup>2</sup> Yunlang Zhang,<sup>6</sup> Rachel Flecker,<sup>2</sup> Emmanuelle Ducassou,<sup>2</sup> Trevor Williams,<sup>2</sup> and the Expedition 401 Scientists<sup>2</sup>

<sup>1</sup>Xu, X., Stine, J., Standing, P., Hernández-Molina, F. J., Billy, I., Chin, S., Feakins, S.J., Li, Z., Mulligan, M., Noto, D., Raad, F., Teixeira, M., Yeon, J., Yousfi, M.Z., Zhang, Y., Flecker, R., Ducassou, E., Williams, T., and the Expedition 401 Scientists, 2026. Data report: X-ray fluorescence scanning of sediment cores, IODP Expedition 401 Site U1610, Gulf of Cádiz, Atlantic. In Flecker, R., Ducassou, E., Williams, T., and the Expedition 401 Scientists, Mediterranean–Atlantic Gateway Exchange. *Proceedings of the International Ocean Discovery Program*, 401: College Station, TX (International Ocean Discovery Program). <https://doi.org/10.14379/iodp.proc.401.203.2026>

<sup>2</sup>Expedition 401 Scientists' affiliations. Correspondence author: [xu.xunhui.72x@st.kyoto-u.ac.jp](mailto:xu.xunhui.72x@st.kyoto-u.ac.jp)

<sup>3</sup>Environnements Paléoenvironnements Océaniques et Continentaux, UMR CNRS 5805, Université de Bordeaux, France.

<sup>4</sup>Department of Earth and Environmental Sciences, University of Iowa, USA.

<sup>5</sup>International Ocean Discovery Program, Texas A&M University, USA.

<sup>6</sup>Department of Earth Sciences, University of Southern California, USA.

## Abstract

International Ocean Discovery Program (IODP) Expedition 401 recovered sediment cores from Site U1610, located in the Gulf of Cádiz. This report presents semiquantitative chemical results based on high-resolution (5 cm) X-ray fluorescence (XRF) scanning of Hole U1610A Miocene to Pliocene core sections from 4.5 to 6 Ma (651–1026 m core depth below seafloor, Method A [CSF-A]). Processed element intensities (counts per second) of Al, Si, Ti, Fe, Rb, Ca, Sr, Zr, Mn, and Ba are discussed. XRF results are divided into four units with depth according to the amplitude and wavelength of cyclicities, among which clear cyclicities with 4–7 m wavelengths are observed in Unit 1. Unit 3 and the upper part of Unit 4 (middle Messinian Salinity Crisis [MSC]) have higher amplitude cyclicity, and Unit 2 (close to the Miocene/Pliocene boundary) and the lower part of Unit 4 (early MSC) have the lowest amplitude signals. The most pronounced spikes of XRF and physical properties occur in the middle of the MSC and at the onset of the MSC. Additionally, this report discusses the implications regarding terrigenous versus biogenic components. There are positive correlations between terrigenous elements (Al, Si, and Ti), but generally weak negative correlations dominate between these terrigenous elements and biogenic elements (Ca and Sr). This high-resolution data set, in conjunction with other data sets produced from Expedition 401, will help with the interpretation of the sedimentary processes and paleoclimate changes impacting the Gulf of Cádiz before, during, and after the MSC.

## 1. Introduction

Marine gateways are oceanic passages (Kennett, 1982; Knutz, 2008) that allow for the exchange of water, heat, salt, nutrients, and biota between oceans and seas (DeConto, 2009). One of the most well-known marine gateways is the Strait of Gibraltar (Figure F1), which currently forms the only connection between the Mediterranean Sea and the Atlantic Ocean. Extreme narrowing of the Miocene Mediterranean–Atlantic connection is thought to have led to the precipitation of the Messinian Salinity Crisis (MSC) salt giant from ~5.97 to 5.33 Ma (Roveri et al., 2014, 2025). The principal objectives of International Ocean Discovery Program (IODP) Expedition 401 were to recover Late Miocene cores from both sides of the Gibraltar Strait that record Mediterranean–

Atlantic exchange and evaluate its impact on regional and global climate. To this end, Miocene–Pliocene sedimentary successions were recovered from two sites west of Portugal (Sites U1385 and U1609), one site in the Gulf of Cádiz (Site U1610), and one site to the east of the Gibraltar Strait in the Alborán Basin (Site U1611) (Figure F1).

The single hole drilled at Site U1610 targeted a complete Late Miocene succession that today lies in the pathway of Mediterranean Overflow Water (MOW) (Iorga and Lozier, 1999; Dietrich et al., 2008; Rogerson et al., 2012a, 2012b). The aims were to use these cores to determine the mechanisms of extreme high-density overflow dynamics, reveal the Late Miocene timing of opening/closure of the Mediterranean–Atlantic gateways (Krijgsman et al., 2018), evaluate the impacts of high-salinity brine from the western Mediterranean on this proximal region west of the gateway (Capella et al., 2017, 2019; Flecker et al., 2025a), and test the existing application of physical theory to the paleoceanography of MOW (Legg et al., 2009; Rogerson et al., 2012a). Drilling at Site U1610 during Expedition 401 reached deeper than 1400 m core depth below seafloor, Method A (CSF-A), significantly exceeding expectations with an 80% recovery rate of Miocene–Pliocene sediments, spanning the age range of interest (Flecker et al., 2025a).

Seven primary lithologies were identified in Hole U1610A, including calcareous clay, calcareous mud, calcareous silty mud, calcareous (sandy) silt(stone), calcareous (silty) sand(stone), clayey calcareous ooze, and dolostone (Flecker et al., 2025a). The primary minerals identified by X-ray diffraction (XRD) analysis of 20 squeeze cake residues include quartz; calcite; feldspars (plagioclase and K-feldspar); clay minerals, including chlorite, mixed-layer illite/smectite (I/S), illite (or mica), and kaolinite; and minor dolomite and pyrite (Flecker et al., 2025a).

Geochemical changes are expected to reflect changes in lithofacies, paleoproductivity, and sediment composition in this region influenced by MOW (Hernández-Molina et al., 2014). X-ray fluorescence (XRF) analysis has been used to document Pleistocene MOW dynamics (Bahr et al., 2015; Moal-Darrigade et al., 2022) and can be used to reconstruct other environmental properties (Hull and Norris, 2011; Croudace et al., 2019). High-resolution scanning of Site U1610 cores was therefore performed to reconstruct how MOW may have evolved during the Messinian in the Gulf of Cádiz. Using a similar methodology to Rothwell and Croudace (2015), this report presents quality controlled XRF data from Site U1610 combined with stratigraphic information to provide an overview of elemental abundance variability. Companion publications describing the XRF data for

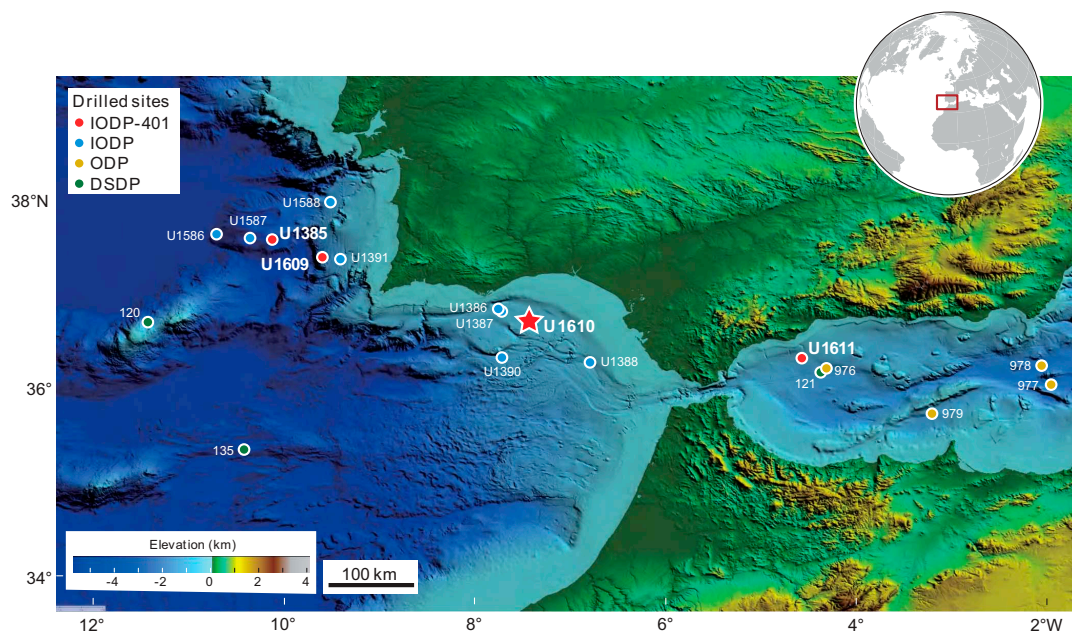


**Figure F1.** Location map of Expedition 401 sites and earlier scientific drilling targets. Star = Site U1610 in Gulf of Cádiz (Flecker et al., 2025a). ODP = Ocean Drilling Program, DSDP = Deep Sea Drilling Project.

Sites U1385 (Raad et al., 2026), U1609 (Teixeira et al., 2026), and U1611 (Standring et al., 2026) are available.

## 2. Methods

Sediment cores from Site U1610 were scanned at the Gulf Coast Repository at Texas A&M University (United States) on the fourth-generation Avaatech Core Scanner (XRF2). The nondestructive method of XRF core scanning uses energy dispersive spectroscopy to simultaneously measure photon energies through fluorescence of major, minor, and trace elements after excitation voltages of 10, 30, and 50 kV are directed at the core surface. Both scanners use a water-cooled 100 W rhodium side Be-window X-ray tube, a Brightspec SiriusSD silicon drift detector, and a Topaz-X high-resolution digital multichannel analyzer (Villa et al., 2024). The measurement window slit size was set at 1 cm downcore by 1.2 cm cross-core. The enclosed prism that houses the detector was continuously flushed with helium to remove natural atmospheric contamination to reduce background noise in the data output.

The XRF data set was measured on the archive section halves of Hole U1610A cores. Measurements were collected every 5 cm, with sample locations occasionally shifted to avoid protruding clasts, cracks, and depressions along the core surface. Each archive section half was scanned at three excitation levels to measure different elements: 10 kV (0.16 mA, 6 s count time; no filter) for major and minor elements (including Al, Si, K, Ca, Ti, Mn, Fe, Cr, P, S, and Mg), 30 kV (1.25 mA, 6 s count time; thick Pd filter) for heavier major and minor elements and geologically relevant trace elements (i.e., Ca, Ti, Mn, Fe, Ni, Sr, Rb, Zr, and Zn), and 50 kV (0.75 mA, 10 s count time; Cu filter) for heavier trace elements (i.e., Sr, Rb, Zr, and Ba).

### 2.1. Sediment core preparation

Prior to scanning, each core section stored at 4°C was warmed up to room temperature to prevent condensation underneath the plastic, which can affect X-ray attenuation (Tjallingii et al., 2007). End caps of the core liners were partially cut and reshaped to allow the detector to fit and measure the first and the last point on the section. Sediment cores were carefully scraped with a glass slide along their width to remove any mold that had grown during storage and to expose a fresh surface. This helped to eliminate contamination from smearing associated with the protective film used during storage. The scraping was performed perpendicular to the core splitting line (parallel to sedimentary bedding) to ensure that no material was moved from its stratigraphic position. The glass slide was wiped clean between scrapes with a laboratory tissue paper (Kimwipes). The core sections were subsequently covered with a 4 µm thick Ultralene XRF film and smoothed to remove air bubbles. The purpose of the film is to prevent contamination as the XRF detector moves down the core. After placement in the XRF core scanner, all sections were leveled to ensure the measurement occurred on a horizontal surface. This was done because any deviation of the surface from 0° can potentially introduce air contamination.

### 2.2. Quality control

To ensure that the XRF scanner was operating correctly, 20 replicate measurements on three standards were run each morning to warm up the scanner, and another set of standards without replicates was run at the end of each day. These standards were utilized to evaluate instrumental bias in acquired count outputs and the operational reliability of the XRF core scanners.

Raw spectral peaks were processed and exported as counts per second for different elements using Brightspec's bAxilBatch software and uploaded into the IODP Laboratory Information Management System (LIMS) database. Quality control of the data involved the deletion of data points that fell into at least one of two categories:

- Sample throughput with values <170,000 counts/s on the 10 kV scan, suggesting that counts of detected elements are too sensitive to the influence of intrinsic errors of the scanner.
- Any data point with a positive Ar value, which indicates that the detector was measuring ambient air rather than the core.

Overall, the typical mean value of argon with a 10 kV scan is around –3760 counts, which signifies little to no atmospheric contamination. Counts values are quite variable from element to element in a single sample with the same voltage and other scan setups (e.g., Ti counts may be significant, whereas Mg counts may not be). Some elements (e.g., Mg and Mo) were measured by the scanner but are not included in this data set because of low detection giving negative or low count values (100–300 counts).

### 3. Results

#### 3.1. XRF stratigraphy of Hole U1610A

The elemental counts have pronounced cyclicity throughout the measured sections and resemble the cyclic patterns observed in the magnetic susceptibility (MS) and natural gamma radiation (NGR) data sets (Figure F2). Some of the broad features of the XRF records mirror those seen in the NGR data; however, there are significant differences, and the extreme peaks evident in the MS data set below 963 m CSF-A are not seen in the XRF results. Gaps in the data set, such as those below 800 m CSF-A in Figure F2, correspond to unrecovered core intervals.

Closer inspection of the data set reveals changes in signal behavior occurring at specific depth intervals. At the top of the core (650–800 m CSF-A), all selected elements have clear cyclicity with a 4–7 m wavelength (Unit 1 in Figure F2). The next interval (800–867 m CSF-A) is characterized by low-amplitude and high-frequency (2 m cycles) signal behavior (Unit 2 in Figure F2) where it includes the Pliocene/Miocene boundary. The amplitude for all elements increases in the 3 m wavelength cycles from 867 to 900 m CSF-A (Unit 3 in Figure F2). This change in cyclicity corre-

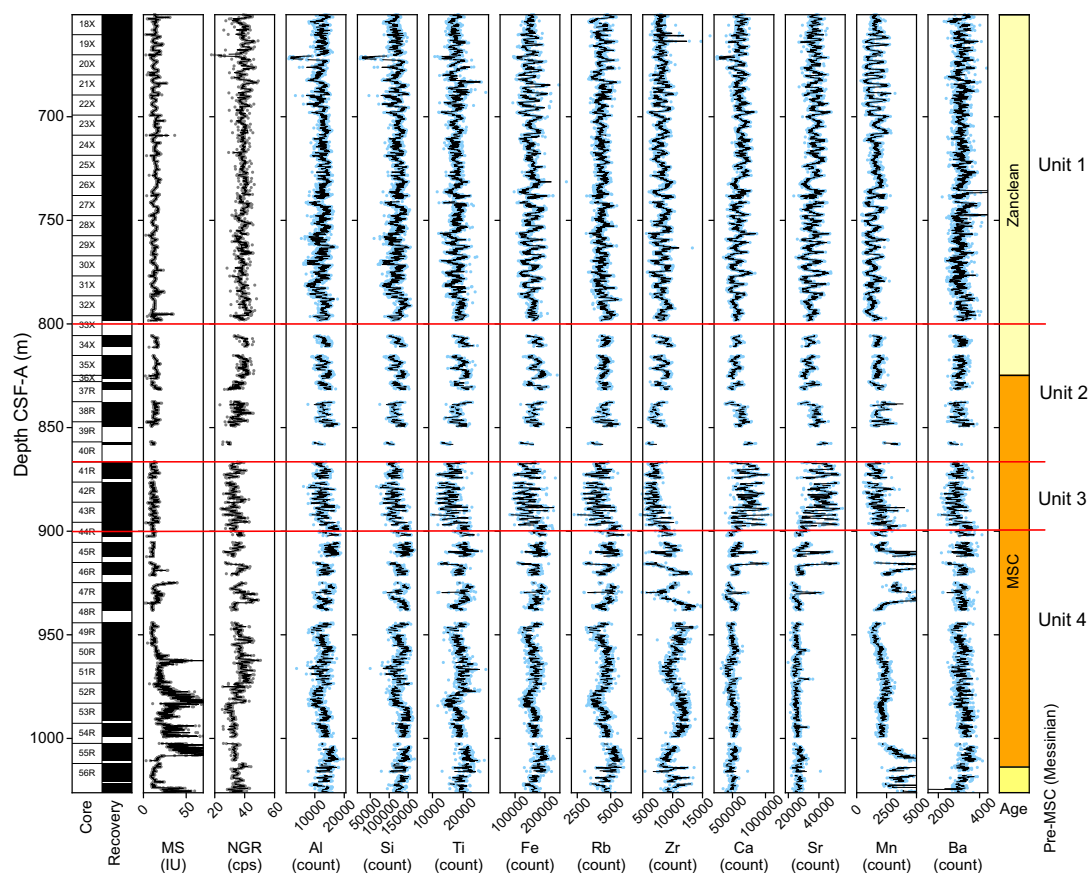


**Figure F2.** Shipboard MS and NGR with select XRF elemental counts, Hole U1610A. Black lines = rolling means (calculated with window size of 3) of shipboard physical properties (MS and NGR) and selected elements. X-axes for select elements and MS results have been adjusted to ensure readability of cyclicities. cps = counts per second.

sponds to a lithology change from a calcareous ooze-rich interval with lighter colors (Unit 3) to the interval of calcareous clay (Unit 2) and the interval comprising abundant calcareous mud with minor coarser and sandy layers (Unit 1). The deepest interval (900–1026 m CSF-A) comprises the lowest-amplitude cycles with high frequency (2 m wavelength cycles), particularly evident in Ca, Ti, Mn, Fe, Rb, Sr, and Zr counts (Unit 4 in Figure F2). Four units are vertically divided by three red horizontal lines located at 800, 867, and 900 m CSF in Figure F2. It is clear that Unit 3 shows a higher amplitude than the other three units, implying larger fluctuations in the supply of terrestrial and biogenic materials before the late MSC at Site U1610. The minor amplitude variations in selected elements within Unit 2 support the inference of stable material input at Site U1610 during the late MSC and shortly thereafter.

Spikes in Ca, Ti, Mn, Rb, Sr, and Zr are evident in the low-amplitude interval of Unit 4. Of these spikes, the greatest relative change is in the counts of Mn (Figure F2). Ca, Sr, and Mn have positive spikes at about 911–930 m CSF-A, mirrored by downward spikes in the NGR data, terrigenous elements (Si, Ti, Fe, Rb, and Zr), and Ba. Amplitudes of these spikes seem to be more pronounced in some biogenic elements (Ca, Sr, and Mn) than the others. Chronological analyses indicate that these geochemical anomalies temporally align with the mid-MSC interval. Below 1012 m CSF-A (corresponding to the onset of the MSC), Rb, Zr, and Mn have pronounced increases in amplitude. Notably, Zr demonstrates an inverse fluctuation pattern relative to Mn within this interval. Below 940 m CSF, some of the terrigenous elements (Al, Si, Ti, Fe, and Rb) present similar trends to NGR but correlate negatively with Zr and biogenic elements (Ca, Sr, and Ba).

Barium has sudden increases at 736 and 747 m CSF-A; however, these spikes do not correspond to any changes in either the other element counts or the physical properties (Figure F2). However, the sharp decline of Ba at 1024 m CSF-A (pre-MSC interval) is synchronous with the abrupt increase in Mn and MS results.

### 3.2. Correlation between elements

The plotted counts of Al, Si, Ti, Ca, Sr, Mn, and Ba (Figure F3) indicate positive correlations between terrigenous elements (Al, Si, and Ti) but generally weak negative correlations between these terrigenous elements and biogenic elements (Ca and Sr). A Spearman's rank correlation for these elements determines the degree and direction of correlation where the data are not normally distributed (Figure F3). For the Site U1610 XRF data, the highest positive correlation is between biogenic elements Ca and Sr (0.88). However, Ca and Sr are poorly correlated with other elements ( $<0.06$ ). Correlation between the two terrigenous elements, Al and Si, is also strongly positive (0.87). Mn is positively correlated with terrigenous elements (Al, Si, and Ti), implying that some Mn is detrital. Ba has a positive but weak correlation (0.47–0.48) with terrigenous elements, indicative of a partial terrigenous origin of Ba.

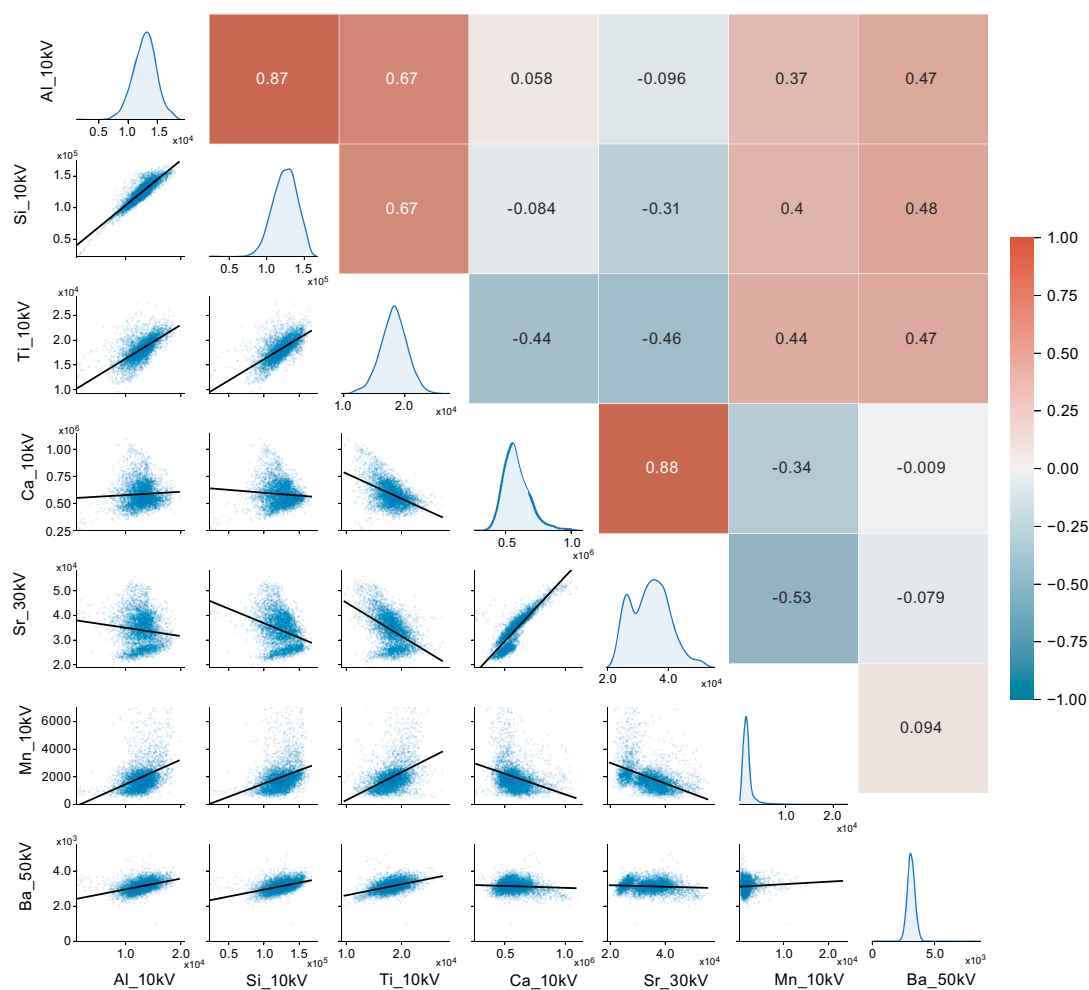


**Figure F3.** Spearman's correlation plot, Hole U1610. Lower left: crossplots between elements (Al, Si, Ti, Ca, Sr, Mn, and Ba). Diagonal kernel density plots illustrate count distribution of each element. Upper right: heat map ranging  $-1$  to  $+1$  (pinks = positive correlations, blues = negative correlations; higher correlation values are reflected in intensity of color).

## 4. Data availability

Data from Expedition 401 data (Flecker et al., 2025b), including the XRF data in this report, are available at Zenodo (<https://zenodo.org/communities/iodp>).

## 5. Acknowledgments

This research used samples provided by the International Ocean Discovery Program (IODP). We are grateful to the crew and technicians on the R/V *JOIDES Resolution* during Expedition 401, as well as the technicians at the Gulf Coast Repository. XRF scans reported here comprise the programmatic scanning for Expedition 401 and were funded by the National Science Foundation (NSF) in agreement with the US Science Support Program (USSSP), including funding for travel support for US Scientists administered by USSSP. Additional travel support for X. Xu was provided by Natural Environment Research Council (NERC) Grant NE/Y005511/1 (Discriminating Deep Water Deposits for IODP Expedition 401: “Mediterranean-Atlantic Gateway Exchange”), Japan Science and Technology Agency (JST) Support for Pioneering Research Initiated by the Next Generation (SPRING) of Kyoto University (Japan) (JPMJSP2110), and Japan Agency for Marine–Earth Science and Technology (JAMSTEC) in participation of Expedition 401 and XRF scanning operations. We thank Jennifer Hertzberg, Laurel Childress, and Vítor Magalhães for their thoughtful assistance in review and edition.

## References

- Bahr, A., Kaboth, S., Jiménez-Espejo, F.J., Sierro, F.J., Voelker, A.H.L., Lourens, L., Röhl, U., Reichart, G.J., Escutia, C., Hernández-Molina, F.J., Pross, J., and Friedrich, O., 2015. Persistent monsoonal forcing of Mediterranean Outflow Water dynamics during the late Pleistocene. *Geology*, 43(11):951–954. <https://doi.org/10.1130/G37013.1>
- Capella, W., Flecker, R., Hernández-Molina, F.J., Simon, D., Meijer, P.T., Rogerson, M., Sierro, F.J., and Krijgsman, W., 2019. Mediterranean isolation preconditioning the Earth System for Late Miocene climate cooling. *Scientific Reports*, 9(1):3795. <https://doi.org/10.1038/s41598-019-40208-2>
- Capella, W., Hernández-Molina, F.J., Flecker, R., Hilgen, F.J., Hssain, M., Kouwenhoven, T.J., van Oorschot, M., Sierro, F.J., Stow, D.A.V., Trabucho-Alexandre, J., Tulbure, M.A., de Weger, W., Yousfi, M.Z., and Krijgsman, W., 2017. Sandy contourite drift in the late Miocene Rifian Corridor (Morocco): reconstruction of depositional environments in a foreland-basin seaway. *Sedimentary Geology*, 355:31–57. <https://doi.org/10.1016/j.sedgeo.2017.04.004>
- Croudace, I.W., Löwemark, L., Tjallingii, R., and Zolitschka, B., 2019. High resolution XRF core scanners: A key tool for the environmental and palaeoclimate sciences. *Quaternary International*, 514:1–4. <https://doi.org/10.1016/j.quaint.2019.05.038>
- DeConto, R.M., 2009. Plate tectonics and climate change. In Gornitz, V., *Encyclopedia of Paleoclimatology and Ancient Environments*. Dordrecht (Springer Netherlands), 784–798. [https://doi.org/10.1007/978-1-4020-4411-3\\_188](https://doi.org/10.1007/978-1-4020-4411-3_188)
- Dietrich, D.E., Tseng, Y.-H., Medina, R., Piacsek, S.A., Liste, M., Olabarrieta, M., Bowman, M.J., and Mehra, A., 2008. Mediterranean Overflow Water (MOW) simulation using a coupled multiple-grid Mediterranean Sea/North Atlantic Ocean model. *Journal of Geophysical Research: Oceans*, 113(C7):C07027. <https://doi.org/10.1029/2006JC003914>
- Flecker, R., Ducassou, E., Williams, T., Amarathunga, U., Balestra, B., Berke, M.A., Blättler, C.L., Chin, S., Das, M., Egawa, K., Fabregas, N., Feakins, S.J., George, S.C., Hernández-Molina, F.J., Krijgsman, W., Li, Z., Liu, J., Noto, D., Raad, F., Rodríguez-Tovar, F.J., Sierro, F.J., Standring, P., Stine, J., Tanaka, E., Teixeira, M., Xu, X., Yin, S., and Yousfi, M.Z., 2025a. Expedition 401 summary. In Flecker, R., Ducassou, E., Williams, T., and the Expedition 401 Scientists, *Mediterranean–Atlantic Gateway Exchange. Proceedings of the International Ocean Discovery Program*, 401: College Station, TX (International Ocean Discovery Program). <https://doi.org/10.14379/iodp.proc.401.101.2025>
- Flecker, R., Ducassou, E., Williams, T., Amarathunga, U., Balestra, B., Berke, M.A., Blättler, C.L., Chin, S., Das, M., Egawa, K., Fabregas, N., Feakins, S.J., George, S.C., Hernández-Molina, F.J., Krijgsman, W., Li, Z., Liu, J., Noto, D., Raad, F., Rodríguez-Tovar, F.J., Sierro, F.J., Standring, P., Stine, J., Tanaka, E., Teixeira, M., Xu, X., Yin, S., and Yousfi, M.Z., 2025b. IODP Expedition 401 X-ray fluorescence (XRF) [Data set]. International Ocean Discovery Program. <https://doi.org/10.5281/zenodo.16459854>
- Hernández-Molina, F.J., Stow, D.A.V., Alvarez-Zarikian, C.A., Acton, G., Bahr, A., Balestra, B., Ducassou, E., Flood, R., Flores, J.-A., Furota, S., Grunert, P., Hodell, D., Jimenez-Espejo, F., Kim, J.K., Krissek, L., Kuroda, J., Li, B., Llave, E., Lofi, J., Lourens, L., Miller, M., Nanayama, F., Nishida, N., Richter, C., Roque, C., Pereira, H., Sanchez Goñi, M.F., Sierro, F.J., Singh, A.D., Sloss, C., Takashimizu, Y., Tzanova, A., Voelker, A., Williams, T., and Xuan, C., 2014. Onset of Mediterranean outflow into the North Atlantic. *Science*, 344(6189):1244–1250. <https://doi.org/10.1126/science.1251306>
- Hull, P.M., and Norris, R.D., 2011. Diverse patterns of ocean export productivity change across the Cretaceous-Paleogene boundary: New insights from biogenic barium. *Paleoceanography*, 26(3). <https://doi.org/10.1029/2010PA002082>
- Iorga, M.C., and Lozier, M.S., 1999. Signatures of the Mediterranean outflow from a North Atlantic climatology: 1. Salinity and density fields. *Journal of Geophysical Research: Oceans*, 104(C11):25985–26009. <https://doi.org/10.1029/1999JC900115>
- Kennett, J.P., 1982. *Marine Geology*: Englewood Cliffs, NJ (Prentice-Hall).
- Knutz, P.C., 2008. Palaeoceanographic significance of contourite drifts. In Rebesco, M., and Camerlenghi, A. (Eds.), *Contourites. Developments in Sedimentology*, 60: (Elsevier), 511–535. [https://doi.org/10.1016/S0070-4571\(08\)10024-3](https://doi.org/10.1016/S0070-4571(08)10024-3)
- Krijgsman, W., Capella, W., Simon, D., Hilgen, F.J., Kouwenhoven, T.J., Meijer, P.T., Sierro, F.J., Tulbure, M.A., van den Berg, B.C.J., van der Schee, M., and Flecker, R., 2018. The Gibraltar Corridor: Watergate of the Messinian Salinity Crisis. *Marine Geology*, 403:238–246. <https://doi.org/10.1016/j.margeo.2018.06.008>
- Legg, S., Briegleb, B., Chang, Y., Chassignet, E.P., Danabasoglu, G., Ezer, T., Gordon, A.L., Griffies, S., Hallberg, R., Jackson, L., Large, W., Özgökmen, T.M., Peters, H., Price, J., Riemenschneider, U., Wu, W., Xu, X., and Yang, J., 2009. Improving oceanic overflow representation in climate models: the gravity current entrainment climate process team. *Bulletin of the American Meteorological Society*, 90(5):657–670. <https://doi.org/10.1175/2008BAMS2667.1>
- Moal-Darrigade, P., Ducassou, E., Giraudeau, J., Bahr, A., Kaboth-Bahr, S., Hanquiez, V., and Perello, M.-C., 2022. MOW strengthening and contourite development over two analog climate cycles (MIS 12–11 and MIS 2–1) in the Gulf of Cadiz: an impact on North Atlantic climate during deglaciation V and MIS 11? *Global and Planetary Change*, 208:103721. <https://doi.org/10.1016/j.gloplacha.2021.103721>
- Raad, F., Standring, P., Le Ber, E., Blättler, C., Billy, I., Chin, S., Teixeira, M., Feakins, S.J., Li, Z., Mulligan, M., Noto, D., Stine, J., Xu, X., Yeon, J., Yousfi, Z.M., Zhang, Y., Flecker, R., Ducassou, E., Williams, T., and the Expedition 401 Scientists, 2026. Data report: X-ray fluorescence scanning of sediment cores, IODP Expedition 401 Site U1385, southwest Iberian margin (Portugal). In Flecker, R., Ducassou, E., Williams, T., and the Expedition 401 Scientists, *Mediterranean–Atlantic Gateway Exchange. Proceedings of the International Ocean Discovery Program*, 401: College Station, TX (International Ocean Discovery Program). <https://doi.org/10.14379/iodp.proc.401.203.2026>

- Rogerson, M., Bigg, G.R., Rohling, E.J., and Ramirez, J., 2012a. Vertical density gradient in the eastern North Atlantic during the last 30,000 years. *Climate Dynamics*, 39(3):589–598. <https://doi.org/10.1007/s00382-011-1148-4>
- Rogerson, M., Rohling, E.J., Bigg, G.R., and Ramirez, J., 2012b. Paleooceanography of the Atlantic-Mediterranean exchange: overview and first quantitative assessment of climatic forcing. *Reviews of Geophysics*, 50(2):RG2003. <https://doi.org/10.1029/2011RG000376>
- Rothwell, R.G., and Croudace, I.W., 2015. Twenty years of XRF core scanning marine sediments: what do geochemical proxies tell us? In Croudace, I.W., and Rothwell, R.G. (Eds.), *Micro-XRF Studies of Sediment Cores: Applications of a non-destructive tool for the environmental sciences*. Dordrecht (Springer Netherlands), 25–102. [https://doi.org/10.1007/978-94-017-9849-5\\_2](https://doi.org/10.1007/978-94-017-9849-5_2)
- Roveri, M., Flecker, R., Krijgsman, W., Lofi, J., Lugli, S., Manzi, V., Sierro, F.J., Bertini, A., Camerlenghi, A., De Lange, G., Govers, R., Hilgen, F.J., Hübscher, C., Meijer, P.T., and Stoica, M., 2014. The Messinian salinity crisis: past and future of a great challenge for marine sciences. *Marine Geology*, 352:25–58. <https://doi.org/10.1016/j.margeo.2014.02.002>
- Roveri, M., Lugli, S., and Manzi, V., 2025. The desiccation and catastrophic refilling of the Mediterranean: 50 years of facts, hypotheses, and myths around the Messinian salinity crisis. *Annual Review of Marine Science*, 17:485–509. <https://doi.org/10.1146/annurev-marine-021723-110155>
- Standring, P., Chin, S., Raad, F., Zhang, Y., Billy, I., Feakins, S.J., Li, Z., Mulligan, M., Noto, D., Stine, J., Teixeira, M., Xu, X., Yeon, J., Yousfi, M.Z., Flecker, R., Ducassou, E., Williams, T., and the Expedition 401 Scientists, 2026. Data report: X-ray fluorescence scanning of sediment cores, IODP Expedition 401 Site U1611, Alborán Sea. In Flecker, R., Ducassou, E., Williams, T., and the Expedition 401 Scientists, *Mediterranean–Atlantic Gateway Exchange. Proceedings of the International Ocean Discovery Program, 401: College Station, TX (International Ocean Discovery Program)*. <https://doi.org/10.14379/iodp.proc.401.204.2026>
- Teixeira, M., Chin, S., Standring, P., Zhang, Y., Billy, I., Feakins, S.J., Li, Z., Mulligan, M., Noto, D., Raad, F., Stine, J., Xu, X., Yeon, J., Yousfi, M.Z., Flecker, R., Ducassou, E., Williams, T., and the Expedition 401 Scientists, 2026. Data report: X-ray fluorescence scanning of sediment cores, IODP Expedition 401 Site U1609, SW Iberia Atlantic margin (Portugal). In Flecker, R., Ducassou, E., Williams, T., and the Expedition 401 Scientists, *Mediterranean–Atlantic Gateway Exchange. Proceedings of the International Ocean Discovery Program, 401: College Station, TX (International Ocean Discovery Program)*. <https://doi.org/10.14379/iodp.proc.401.201.2026>
- Tjallingii, R., Röhl, U., Kölling, M., and Bickert, T., 2007. Influence of the water content on X-ray fluorescence core-scanning measurements in soft marine sediments. *Geochemistry, Geophysics, Geosystems*, 8(2):Q02004. <https://doi.org/10.1029/2006GC001393>
- Villa, A., Amadori, C., Borrelli, C., Christeson, G., Estes, E., Guertin, L., Hertzberg, J., Kaplan, M.R., Koorapati, R.K., Lam, A.R., Lowery, C.M., McIntyre, A., Reece, J., Robustelli Test, C., Routledge, C.M., Standring, P., Sylvan, J.B., Thompson, M., Wang, Y., Wee, S.Y., Williams, T., Yeon, J., Teagle, D.A.H., Coggon, R.M., and the Expedition 390/393 Scientists, 2024. Data report: X-ray fluorescence scanning of sediment cores, IODP Expedition 390/393 Site U1558, South Atlantic Transect. In Coggon, R.M., Teagle, D.A.H., Sylvan, J.B., Reece, J., Estes, E.R., Williams, T.J., Christeson, G.L., and the Expedition 390/393 Scientists, *South Atlantic Transect. Proceedings of the International Ocean Discovery Program, 390/393: College Station, TX (International Ocean Discovery Program)*. <https://doi.org/10.14379/iodp.proc.390393.203.2024>